Size and Shape of Detergent Micelles Determined by Small-Angle X-ray Scattering

Jan Lipfert,[†,‡] Linda Columbus,[§,⊗] Vincent B. Chu,[||,‡] Scott A. Lesley,[§,#] and Sebastian Doniach*[,†,||,‡,⊥]

Departments of Physics and Applied Physics, Biophysics Program, and Stanford Synchrotron Radiation Laboratory, Stanford University, Stanford, California 94305, Unité Biochimie Structurale, Institut Pasteur, 75724 Paris, France,[§]The Joint Center of Structural Genomics and The Scripps Research Institute, Department of Molecular Biology, La Jolla, California 92037, and The Genomics Institute of the Novartis Research Foundation, San Diego, California 92121

Received: April 18, 2007; In Final Form: August 16, 2007

We present a systematic analysis of the aggregation number and shape of micelles formed by nine detergents commonly used in the study of membrane proteins. Small-angle X-ray scattering measurements are reported for glucosides with 8 and 9 alkyl carbons (OG/NG), maltosides and phosphocholines with 10 and 12 alkyl carbons (DM/DDM and FC-10/FC-12), 1,2-dihexanoyl-*sn*-glycero-phosphocholine (DHPC), 1-palmitoyl-2-hydroxy-*sn*-glycero-3-[phospho-*rac*-(1-glycerol)] (LPPG), and 3-[(3-cholamidopropyl)dimethylammonio]-1-propane sulfonate (CHAPS). The SAXS intensities are well described by two-component ellipsoid models, with a dense outer shell corresponding to the detergent head groups and a less electron dense hydrophobic core. These models provide an intermediate resolution view of micelle size and shape. In addition, we show that Guinier analysis of the forward scattering intensity can be used to obtain an independent and model-free measurement of the micelle aggregation number and radius of gyration. This approach has the advantage of being easily generalizable to protein−detergent complexes, where simple geometric models are inapplicable. Furthermore, we have discovered that the position of the second maximum in the scattering intensity provides a direct measurement of the characteristic head group−head group spacing across the micelle core. Our results for the micellar aggregation numbers and dimensions agree favorably with literature values as far as they are available. We de novo determine the shape of FC-10, FC-12, DM, LPPG, and CHAPS micelles and the aggregation numbers of FC-10 and OG to be ca. 50 and 250, respectively. Combined, these data provide a comprehensive view of the determinants of micelle formation and serve as a starting point to correlate detergent properties with detergent−protein interactions.

Introduction

Micelle forming detergents are important in a range of scientific and technological applications. In particular, they are used frequently in biochemical studies as a mimetic of cell membranes to solubilize integral membrane proteins.[1−3] An understanding of detergent properties is desired to determine optimal detergent conditions for extraction, purification, and structural and functional characterization of membrane proteins.[3−6] Even though the presence of the protein component in a protein−detergent complex (PDC) will in general alter detergent packing with respect to the "detergent only" micelles,[7−9] characterization of detergent micelles can reveal intrinsic detergent packing preferences that have a direct influence on protein−detergent interactions. More specifically, recent results suggest that the packing preferences of different detergents have an influence on the conformation of membrane spanning helices buried in their respective micelles.[10] The observation that detergent micelle geometry can influence the conformation of proteins buried in their hydrophobic core is reminiscient of the fact that lipid packing preferences can impact membrane protein function in lipid bilayers.[11] While quantitative models of bilayer deformation and packing have been obtained,[11] such models are lacking for detergent micelles at the present. Accurate measurements of the properties of micelles formed by a single detergent species can serve as a starting point to correlate detergent packing preferences with trends in protein−detergent interactions, to calibrate theories of micellization,[12,13] and to understand more complicated detergent mixtures and their interactions with proteins.

Here, we use small-angle X-ray scattering (SAXS) as a powerful probe of detergent micelles. Small-angle scattering can provide insight into the size, shape, and interactions of biological macromolecules, polymers, and detergent systems in solution.[2,14−17] Both small-angle neutron scattering (SANS)[18−24] and SAXS[25−27] have been used to study the solution structure and interactions of detergent micelles.

We present SAXS measurements for nine detergents commonly used in membrane protein studies (see Table 1). The set includes glucosides with 8 and 9 alkyl carbons (OG/NG), and maltosides and phosphocholines with 10 and 12 alkyl carbons (DM/DDM and FC-10/FC-12). Furthermore, the study comprises 1,2-dihexanoyl-*sn*-glycero-phosphocholine (DHPC), which has two alkyl chains, the ionic detergent 1-palmitoyl-2-hydroxy-

* Address correspondence to this author. E-mail: doniach@drizzle.stanford.edu, Phone: +1-650-723-4786. Fax: +1-650-725-2189.
[†] Department of Physics, Stanford University.
[||] Department of Applied Physics, Stanford University.
[⊥] Biophysics Program and Stanford Synchrotron Radiation Laboratory, Stanford University.
[‡] Institut Pasteur.
[§] The Joint Center of Structural Genomics and The Scripps Research Institute.
[#] The Genomics Institute of the Novartis Research Foundation.
[⊗] Current address: Department of Chemistry, University of Virginia, Charlottesville, VA 22901.

10.1021/jp073016l CCC: $37.00
Published on Web 10/09/2007

TABLE 1: Detergent Properties

detergent (abbreviation)	ionic property	FW[a] (Da)	cmc[a] (mM)	V_{mon}[b] (Å^3)	ρ_{det}[c] (e/Å^3)	N[d] (lit.)	$N_{Guinier}$[d] (eq 4)	N_{core}[d] (eq 10)	R_g[e] (Å)
n-decylphosphocholine (FC-10)	zwitterionic	323	11[h]	494.3	0.360	NR[g]	45−50	50−53	25.5 ± 1.0
n-dodecylphosphocholine (FC-12)	zwitterionic	351	1.5[h]	548.1	0.354	50−60,[8] 70−80[40]	60−70	75−80	34.0 ± 2.0
n-decyl-β-D-maltoside (DM)	non-ionic	483	1.8[h]	644.0	0.407	69[h]	82−86	85−90	27.0 ± 0.5
n-dodecyl-β-D-maltoside (DDM)	non-ionic	511	0.17[h]	697.8	0.398	78−149,[h] 140[55]	135−140	135−145	35.0 ± 1
n-octyl-β-D-glucoside (OG) (50 mM)	non-ionic	292	18[57]−23[58]	418.6	0.382	27−100,[57] 87[43]	80−85	100	30.0 ± 3.0
n-nonyl-β-D-glucoside (NG) (10 mM)	non-ionic	306	6.5[59]	445.5	0.377	NR[g]	240−260	230−250	43.0 ± 5.0
n-decyl-β-D-glucoside (DG)	non-ionic	320	2.2[60]	472.4	0.373	200−400[46]	ND[f]	ND[f]	ND
1,2-dihexanoyl-*sn*-glycerophosphocholine (DHPC)	zwitterionic	453	14−15[42]	677.2	0.363	27,[41] 35[42]	35−40	25−35	19.0 ± 1.0
1-palmitoyl-2-hydroxy-*sn*-glycero-3-[phospho-*rac*-(1-glycerol)] (LPPG)	ionic	507	0.018[61]	692.8	0.395	≈125[41]	160−170	160−170	37.0 ± 2.0
3-[(3-cholamidopropyl)-dimethylammonio]-1-propane sulfonate (CHAPS) (25 mM)	zwitterionic	615	8.0[62]	830.3	0.405	10[62]	11−12	16−17[i]	16.0 ± 1.0

[a]Formula weights of the detergent monomers (FW) and critial micelle concentrations (cmc) were taken from the literature. [b]Monomer volumes (V_{mon}) were calculated from published specific densities,[8] using the Tanford formula for alkyl chain volumes to adjust for different chain lengths.[38] For LPPG, the molecular volume was computed by summing the partial chemical group volumes reported by Reynolds and McCaslin.[39] [c]The detergent electron density values (ρ_{det}) were computed by summing the number of electrons from the chemical composition and dividing by the molecular volume. [d]Micellar aggregation numbers (N) were taken from the literature as far as available and determined from the forward scattering intensity ($N_{Guinier}$, eq 4) and from the hydrophobic core volumes (N_{core}, eq 10) (see text). [e] Radii of gyration (R_g) were obtained from Guinier fits to the SAXS data (see text). [f] ND, no data were obtained for this detergent [g] NR, no reference was available. [h] Anatrace, Inc. [i] For CHAPS, a one-component ellipsoid model was fit to the scattering data (see text).

sn-glycero-3-[phospho-*rac*-(1-glycerol)] (LPPG), which features a 15 carbon alkyl chain, and 3-[(3-cholamidopropyl)dimethylammonio]-1-propane sulfonate (CHAPS), which does not have an alkyl chain, but a steroid-like hydrophobic group.

In this study we present three complementary analyses of the SAXS data. First, we show that the forward scattering intensity obtained from Guinier analysis of the very low angle scattering data can be used to determine the micelle aggregation number N (i.e., the number of detergent monomers in a micelle). This measurement does not require fitting of geometrical parameters to the scattering data and makes no assumptions about the shape or geometry of the micelle. An advantage of this approach is that it can be generalized in a straightforward manner to protein−detergent complexes,[2] where the fitting of a form factor model is complicated by the fact that the structure of the protein in the PDC is a priori unknown.

Second, we fit the full scattering profiles with a two-shell ellipsoid form factor model. In this two-component model the electron dense outer shell corresponds to the detergent head groups and the less electron dense core corresponds to the hydrophobic interior of the micelles. This approach is similar to previous studies that model micelles using simple geometric shapes, such as two-component spheres,[18] ellipsoids,[19,20,22,25] or cylinders[26] whose parameters are fit against the experimental data. While still a significant simplification, these models can provide a comprehensive picture of the size and shape of detergent micelles.[24,28] The hydrophobic core volume computed from the ellipsoid model provides an independent estimate of the aggregation number and we find good agreement with the values obtained from the forward scattering intensity, and with literature values as far as they are available.

Third, we observe that the position of the second maximum of the SAXS intensity observed for detergents with alkyl tail groups is a direct measurement of the head group−head group spacing across the micelle. Determination of the characteristic head group−head group distance from the position of the second maximum in the scattering intensity is straightforward and robust and the results are in good agreement with the parameters derived from the two-component ellipsoid models. This characteristic distance across the micelle likely constrains detergent−protein interactions and appears to be a determinant of protein conformational homogeneity inside of micelles.[10]

Taken together, our results provide a comprehensive data set of micelle sizes and shapes for detergents commonly used in membrane protein studies. The data highlight trends for micelle size and shape across different detergents and provide insight into the different contributions to the free energy of micelle formation.

Materials and Methods

SAXS Data Collection. SAXS data were measured at the XOR/BESSRC undulator beam line 12-ID of the Advanced Photon Source, Argonne, IL, employing a sample−detector distance of 2 m and a X-ray phosphor detector optically coupled to a 3 × 3 mosaic CCD. The data were collected with a custom-made thermo-controlled sample holder[29] at a temperature of 25 °C and an X-ray energy of 12 keV (corresponding to a wavelength of $\lambda = 1$ Å). The usable range of momentum transfer q was $0.022 < q < 0.28$ Å^{-1} ($q = 4\pi \sin(\theta)/\lambda$, where 2θ is the total scattering angle and λ is the X-ray wavelength). Further details of the measurement and beamline are as described.[29−31]

DM, DDM, FC-10, FC-12, OG, NG, DG, and CHAPS were purchased from Anatrace. LPPG and DHPC were purchased from Avanti Polar Lipids. Data were collected at detergent concentrations of 5, 10, 25, 50, 75, 100, 150, and 200 mM (except for OG, FC-10, and CHAPS, where a profile at 200 mM was not recorded) with 20 mM phosphate buffer, pH 6.2, and 150 mM NaCl. Each detergent concentration series was prepared from a 1 M stock solution. For DG only a limited set of data at detergent concentrations of 12.5, 25, and 50 mM was obtained with the same buffer conditions.

We employed 8 mg/mL horse heart cytochrome *c* (Sigma), in 100 mM acetate buffer, pH 4.6, with 0.5 M guanidinium hydrochloride and 1 mg/mL of a 24mer DNA duplex (prepared as described in ref 32) suspended in 50 mM Na-MOPS, pH 7.0, with 150 mM NaCl as molecular weight standards. All samples were centrifuged at 11000 × g for 10 min prior to data collection. For each condition, 5 exposures of 0.1 s each were taken, image corrected, and circularly averaged. The 5 resulting profiles for each condition were averaged to improve signal

quality. Appropriate buffer profiles were collected with identical procedures and subtracted for background correction. We have observed radiation damage for proteins and some detergents (in particular with sugar-based head groups) using the SAXS setup at beam line 12-ID at the APS with integration times ≥ 1.0 s, therefore, the total exposure time was limited to 0.5 s for all measurements in this study. The absence of radiation damage was confirmed by comparing subsequent exposures of the same sample, and no significant changes were detected (data not shown).

SAXS Theory. For monodisperse solutions of approximately spherical particles (spherical on the length scale of the interparticle spacing), the measured scattering intensity as a function of momentum transfer q is given by[15,24]

$$I(q) = cP(q)S(q,c) \tag{1}$$

c is the particle concentration, $P(q)$ is the form factor (also known as particle structure factor), and $S(q,c)$ is the solution structure factor. $P(q)$ corresponds to the orientationally averaged scattering profile of a single particle and can be computed from a structural model. $S(q,c)$ accounts for particle interactions in solution and modifies the measured scattering profile at finite concentrations.[15,19,33,34] The solution structure factor $S(q,c)$ modifies $I(q)$ most strongly at small momentum transfer q. $S(q,c)$ can in principle be computed, at least approximatively, from solution theory.[28,33,34] For weakly interacting particles at low enough concentrations, $S(q,c)$ is equal to unity and the scattering intensity is given by the particle form factor alone.

In the limit that interparticle correlations are negligible, the scattering intensity for very low momentum transfer q is given by the Guinier approximation[35,36]

$$I(q) \approx I(0) \exp(-R_g^2 q^2/3) \tag{2}$$

The forward scattering intensity $I(0)$ and radius of gyration R_g are obtained by fitting a straight line to a plot of $\ln(I)$ as a function of q^2. The Guinier approximation is valid only for small qR_g. In practice, reliable fits can be obtained by using a q range such that $qR_g < 1.3$.[15] Guinier fits presented in this work use a fitting range such that $qR_g < 1.2$, and errors are determined by varying the fitting range in steps of $q = 0.0025$ Å^{-1}.

In the absence of interparticle interference effects, the forward scattering intensity is proportional to the square of the total scattering contrast[15,36]

$$I(0) = Kc[V(\rho - \rho_s)]^2 \tag{3}$$

For X-ray scattering, the total scattering contrast is $V(\rho - \rho_s)$, where V is the molecular volume, ρ is the average electron density of the particle (equal to the total number of electrons in the particle divided by V), and ρ_s is the electron density of the solvent. The solvent in our experiments is 20 mM phosphate buffer with 150 mM NaCl added and $\rho_s = 0.34$ e/Å^3.[37] K is a proportionality constant that can be determined from the measurement of a molecular weight standard of known concentration, molecular volume, and electron density.

It is a direct consequence of eq 3 that a micelle composed of N detergent monomers scatters N-fold more strongly in the forward direction than N monomers (as the concentration of the micelle is reduced by $1/N$, but the molecular volume N-fold increased). Therefore, we can determine the micellar aggregation number by comparing the measured $I(0)_{det}$ (from Guinier analysis) to that expected for a detergent monomer

$$N = \frac{I(0)_{det}}{I(0)_{mon}} = \frac{I(0)_{det}}{K(c - \mathrm{cmc})(\rho_{det} - \rho_s)^2 V_{mon}^2} \tag{4}$$

V_{mon} is the molecular volume of a detergent monomer. Monomer volumes were calculated from published specific densities,[8] using the Tanford formula for alkyl chain volumes to adjust for different chain lengths.[38] For LPPG, the molecular volume was computed by summing the partial chemical group volumes reported by Reynolds and McCaslin.[39] Detergent electron densities ρ_{det} were computed by summing the number of electrons from the chemical composition and dividing by the molecular volume. V_{mon} and ρ_{det} values are reported in Table 1. The proportionality constant K was determined from measurements of cytochrome c and a 24 bp DNA duplex as molecular weight standards (see "SAXS Data Collection"). K values from both standards deviate by less than 3% (data not shown) and in the following the cytochrome c results are used.

Form Factor Models. The X-ray scattering amplitude of a particle with electron density $\rho(\mathbf{r})$ is given by

$$A(\mathbf{q}) = \int (\rho(\mathbf{r}) - \rho_s) \exp(i\mathbf{q}\cdot\mathbf{r})\, \mathrm{d}^3\mathbf{r} \tag{5}$$

and the particle form factor is equal to the square of the amplitude, averaged over all orientations, $P(q) = \langle |A(q)|^2 \rangle_\Omega$. For a sphere of uniform electron density ρ and radius R the scattering amplitude is[15,28,35]

$$A_{sph}(q) = 3V_{sph}(\rho - \rho_s)\frac{\sin(qR) - qR\cos(qR)}{(qR)^3} = 3V_{sph}(\rho - \rho_s)\frac{j_1(qR)}{qR} \tag{6}$$

where $V_{sph} = 4\pi R^3/3$ is the volume of the sphere and j_1 is the first-order spherical Bessel function. The scattering amplitude for a spheroid with one semi-axis of length a and two semi-axes of length b is related to that of the sphere by replacing qR in eq 6 with $u = q(x^2a^2 + (1 - x^2)b^2)^{1/2}$, where x is the cosine of the angle between the axis $\hat{a}$ and the vector $\mathbf{q}$ and the final result has to be integrated over all values of x. For a two-shell sphere or ellipsoid, the scattering amplitude is computed by adding the contributions for each shell. In particular, for a two-shell ellipsoid with a core of density ρ_1 and one semi-axis a and two core semi-axes b and an outer shell of density ρ_2 and thickness t_a and t_b in the a and b dimensions (see Figure 1) the particle form factor is given by

$$P(q) = \int_0^1 \left(3V_1(\rho_1 - \rho_2)\frac{j_1(u_1)}{u_1} + 3(V_1 + V_2)(\rho_2 - \rho_s)\frac{j_1(u_2)}{u_2}\right)^2 \mathrm{d}x \tag{7}$$

with $u_1 = q(a^2x^2 + b^2(1 - x^2))^{1/2}$, $u_2 = q((a + t_a)^2x^2 + (b + t_b)^2(1 - x^2))^{1/2}$, the core volume $V_1 = 4\pi ab^2/3$, and the total volume $V_1 + V_2 = 4\pi(a + t_a)(b + t_b)^2/3$. For $a < b$ the spheroid is *oblate* and for $a > b$ it is *prolate*. The ellipticity ϵ is a useful quantity for characterizing how spherical or elongated an ellipsoid is, $\epsilon = (1 - (a/b)^2)^{1/2}$ for oblate and $\epsilon = (1 - (b/a)^2)^{1/2}$ for prolate shapes.

The radius of gyration for a particle with electron density $\rho(\mathbf{r})$ is given by

$$R_g^2 = \left(\int r^2(\rho(\mathbf{r}) - \rho_s)\, \mathrm{d}^3r\right)/\left(\int (\rho(\mathbf{r}) - \rho_s)\, \mathrm{d}^3r\right) \tag{8}$$

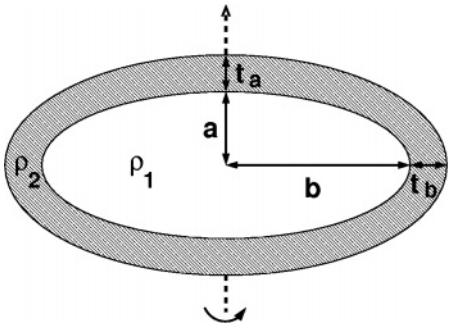

Figure 1. Schematic of the two-component ellipsoid model. The rotation symmetry axis is shown as a dashed line. a and b are the dimensions and ρ_1 the electron density of the hydrophobic core. t_a and t_b are the thickness and ρ_2 the electron density of the head group region. The figure shows the case of an oblate ellipsoid with $a < b$, for $a > b$ the ellipsoid is prolate.

For the two-component spheroid model eq 8 can be evaluated and the result is

$$R_g^2 = \frac{1}{5}\frac{(\rho_2-\rho_s)(a+t_a)(b+t_b)^2[(a+t_a)^2+2(b+t_b)^2]+(\rho_1-\rho_2)ab^2(a^2+2b^2)}{(\rho_2-\rho_s)(a+t_a)(b+t_b)^2+(\rho_1-\rho_2)ab^2} \quad (9)$$

Results and Discussion

SAXS profiles were measured at different detergent concentrations for all nine detergents included in this study as described in Material in Methods. Below the critical micelle concentration (cmc, Table 1), detergent molecules remain monomeric in solution and do not form micelles.[38] For a given total detergent concentration c, the concentration of detergent molecules participating in micelles is approximately (c − cmc). No significant scattering signal was detected for any of the investigated detergents at concentrations below the cmc (data not shown), indicating that the scattering from individual solvated detergent monomers is very weak. Therefore, scattering profiles below (or very close to) the cmc are excluded in the following analysis. Scattering intensities are shown as a function of momentum transfer q for different detergent concentrations in Figures 2A−10A.

For concentrations low enough so that interparticle interference effects are negligible (typically ≤50 mM, see below) scattering profiles for all detergents except for the glucosides are virtually superimposable after rescaling by (c − cmc) (data not shown). This and the fact that the data show good linearity in the Guinier region (see below) for low detergent concentrations indicate that the micelle distributions are approximately monodisperse, in good agreement with previous results for the non-ionic detergents DHPC[20] and DDM.[25]

Determination of Aggregation Numbers from Guinier Analysis. Forward scattering intensities $I(0)$ and radii of gyration R_g for the nine detergents included in this study were obtained from Guinier analysis (eq 2) of the low q scattering data. Guinier fits are shown in Figures 2B−10B. In general, the fitted R_g and $I(0)$ are expected to be functions of detergent concentration, as (1) the size of the detergent micelles is known to increase with c and since (2) interparticle interference modifies the scattering profiles for high c, which leads to changes in the apparent R_g and $I(0)$. To probe the effects of increasing concentration and to obtain reliable estimates of the micellar R_g and $I(0)$, Guinier analysis of scattering profiles collected at different concentrations was performed. The apparent aggregation numbers obtained from eq 4 are shown as a function of (c − cmc) in Figures 2C−10C. Additionally, the measured scattering profiles were linearly extrapolated to zero concentration (thus treating interparticle interference and effects of the detergent concentration on micelle size to second order in c). The aggregation numbers from Guinier analysis of the extrapolated profile are shown as black symbols at zero concentration in Figures 2C−10C.

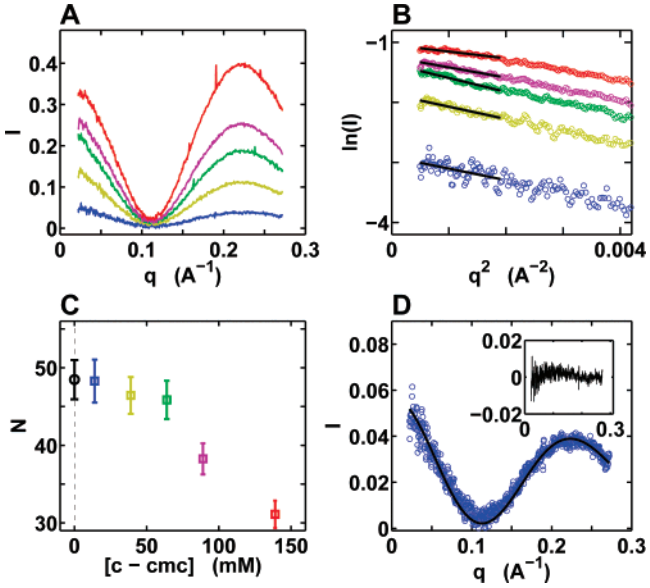

Figure 2. Scattering data, Guinier analysis, and two-shell ellipsoid fit for FC-10. (A) SAXS profiles ($I(q)$) of FC-10 at detergent concentrations of 25 (blue), 50 (brown), 75 (green), 100 (purple), and 150 (red) mM. Profiles at 5 and 10 mM were recorded, but at these detergent concentrations below the cmc scattering was not detectable within experimental error. (B) Guinier representation (ln(I) as a function of q^2) of the low angle data (same color code as part A) and Guinier fits (black lines). The increase in scattering signal (decrease in scatter) with increasing concentration is observed. (C) Apparent aggregation numbers N obtained from the extrapolated forward scattering intensity and eq 4 (squares, same color code as in part A). The point at 0 mM (black circle) corresponds to the estimate obtained by linearly extrapolating the measured profiles to zero concentration. Errors are obtained from repeat fits with different fitting ranges and by propagating the error from repeat measurements of the molecular weight standard. (D) Two-component ellipsoid fit (black solid line) and scattering intensity recorded at 25 mM detergent concentration (blue circles). The residuals of the fit are shown in the inset. Fitted parameters are presented in Table 2.

We find that for low detergent concentrations (typically $c \leq$ 50 mM) the apparent values for N (and R_g, not shown) are independent, within experimental errors, of detergent concentration, except for OG and CHAPS. Furthermore, the apparent aggregation numbers at low detergent concentrations agree with the values obtained from Guinier analysis of the extrapolated scattering profile. These results indicate that for the lowest detergent concentrations used in our measurements interparticle interference effects are negligible and micelle aggregation numbers are relatively independent of detergent concentration. The radii of gyration and micelle aggregation numbers obtained from eq 4 at these low detergent concentrations are reported in Table 1.

The only exceptions are OG and to a lesser extent NG and CHAPS, for which the micelles seem to grow significantly with increasing detergent concentration. The alkyl-glucosides and CHAPS results are discussed in more detail in the next section.

The changes in apparent aggregation number or $I(0)$ (in addition to the trivial linear dependence of $I(0)$ on c) for high c can reveal the nature of intermicellar interactions. An observed increase in forward scattering intensity with increasing c is

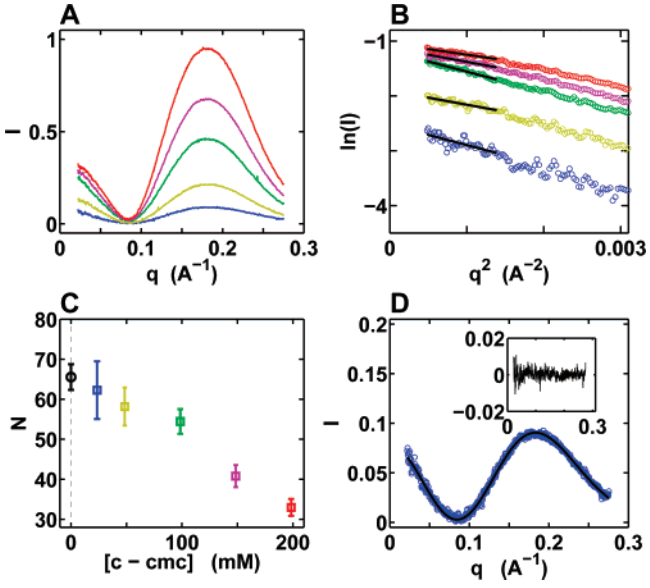

Figure 3. Scattering data, Guinier analysis, and two-shell ellipsoid fit for FC-12. (A) SAXS profiles ($I(q)$) of FC-12 at detergent concentrations of 25 (blue), 50 (brown), 100 (green), 150 (purple), and 200 (red) mM. Profiles at 5 and 10 mM were recorded and a weak scattering signal was detected; however, the signal-to-noise ratio of the data did not allow for a reliable Guinier fit and these profile were excluded from the analysis. (B) Guinier representation ($\ln(I)$ as a function of q^2) of the low angle data (same color code as part A) and Guinier fits (black lines). The increase in scattering signal (decrease in scatter) with increasing concentration is apparent. (C) Apparent aggregation numbers N obtained from the extrapolated forward scattering intensity and eq 4 (squares, same color code as in part A). The point at 0 mM (black circle) corresponds to the estimate obtained by linearly extrapolating the measured profiles to zero concentration. (D) Two-component ellipsoid fit (black solid line) and scattering intensity recorded at 25 mM detergent concentration (blue circles). The residuals of the fit are shown in the inset. Fitted parameters are presented in Table 2.

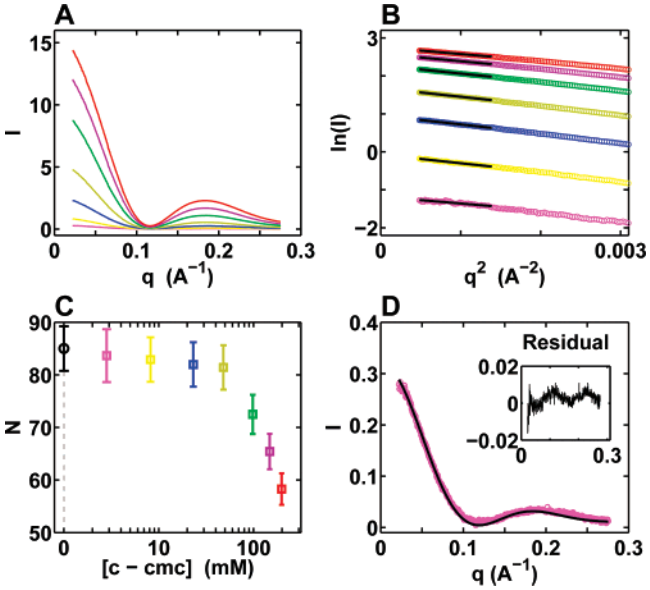

Figure 4. Scattering data, Guinier analysis, and two-shell ellipsoid fit for DM. (A) SAXS profiles ($I(q)$) of DM at detergent concentrations of 5 (magenta), 10 (yellow), 25 (blue), 50 (brown), 100 (green), 150 (purple), and 200 (red) mM. (B) Guinier representation ($\ln(I)$ as a function of q^2) of the low angle data (same color code as part A) and Guinier fits (black lines). (C) Apparent aggregation numbers N obtained from the extrapolated forward scattering intensity and eq 4 (squares, same color code as in part A). The point at 0 mM (black circle) corresponds to the estimate obtained by linearly extrapolating the measured profiles to zero concentration. Note the logarithmic scale. (D) Two-component ellipsoid fit (black solid line) and scattering intensity recorded at 5 mM detergent concentration (magenta circles). The residuals of the fit are shown in the inset. Fitted parameters are presented in Table 2.

indicative of interparticle attraction and/or growing micelles, as observed for the alkyl-glucosides and CHAPS. A decrease of $I(0)$ with increasing c is expected if interparticle repulsion[15] is the dominant effect at higher concentrations. For all detergents investigated, except for the alkyl-glucosides and CHAPS, the apparent $I(0)$ decreased with increasing concentrations at high c, indicative of interparticle repulsion, presumably due to excluded volume effects. For LPPG, the only charged detergent in this study, the decrease in forward scattering intensity with increasing c is particularly pronounced and can likely be attributed to electrostatic repulsion.

Two-Component Ellipsoid Models. The results of the Guinier analysis indicate that interparticle interference is negligible for the lowest detergent concentrations used in our experiments. Under these conditions, the solution structure factor $S(q,c)$ in eq 1 is equal to unity and the scattering data can be described by using a model for the particle form factor $P(q)$.

We employ a two-shell ellipsoid model for the form factor (eq 7 in Materials in Methods) to fit the scattering intensity. The model features an ellipsoidal core with one semi-axis a, two semi-axes b, and electron density ρ_1, representing the hydrophobic interior of the micelle, and an outer shell of thickness t_a and t_b in the a and b dimensions and electron density ρ_2, corresponding to the detergent head groups (Figure 1).

It has been shown that the alkyl chains in the hydrophobic core of detergent micelles are closely packed and that the core contains no or very little water.[24,38] ρ_1 can, therefore, be computed by dividing the number of electrons per alkyl chain by the monomer alkyl chain volume V_{tail}. For a chain of n_c alkyl carbons, V_{tail} is given by the Tanford formula[38] $V_{tail} = (27.4 + 26.9n_c)$ Å ^{3}. An estimate for ρ_2 can be obtained by dividing the number of electrons in the detergent head group by the head group volume, which is computed as $(V_{mon} - V_{tail})$; however, this approximation neglects the effects of hydration (see below).

We employ a nonlinear least-squares fitting routine implemented in Matlab (Mathworks) to fit two-component spheres and prolate and oblate ellipsoids to the scattering data. As the information about the absolute scattering intensity is already used in the Guinier analysis, the form factor model is fit to the shape of the scattering profile up to an arbitrary scaling constant. Fitting parameters are a, b, and the head group thickness $t_a = t_b$. Additionally, we investigate whether varying t_a and t_b independently and whether treating the head group layer density ρ_2 as a free parameter alter the fit. Micelle aggregation numbers can be computed from the form factor models by dividing the total volume of the dry hydrophobic core by the volume per monomer.[20,25−27]

$$N_{core} = \frac{4}{3}\pi ab^2/V_{tail} \qquad (10)$$

FC-10, FC-12, and DHPC. The scattering profiles of the phosphocholines FC-10, FC-12, and DHPC are well modeled by two-component prolate ellipsoid form factors. The fitted parameters are presented in Table 2, and scattering profiles and fits are shown in Figures 2D, 3D, and 8D. Varying ρ_2 or t_a and t_b independently did not significantly improve the fits, and gave values for t_b within 0.4 Å of t_b. The small value for the thickness of the head group layer, $t_a \approx 3$ Å for both FC-10 and FC-12, suggests that the head group adopts a compact conformation, likely with the negatively charged phosphate group in close

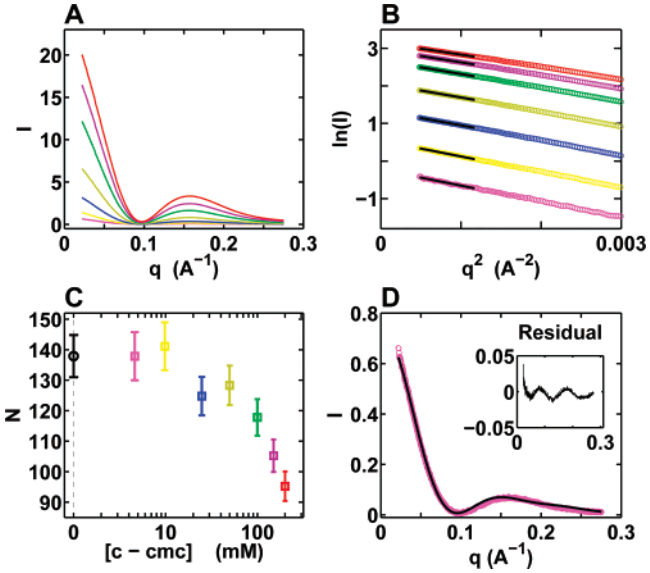

Figure 5. Scattering data, Guinier analysis, and two-shell ellipsoid fit for DDM. (A) SAXS profiles ($I(q)$) of DDM at detergent concentrations of 5 (magenta), 10 (yellow), 25 (blue), 50 (brown), 100 (green), 150 (purple), and 200 (red) mM. (B) Guinier representation ($\ln(I)$ as a function of q^2) of the low angle data (same color code as part A) and Guinier fits (black lines). (C) Apparent aggregation numbers N obtained from the extrapolated forward scattering intensity and eq 4 (squares, same color code as in part A). The point at 0 mM (black circle) corresponds to the estimate obtained by linearly extrapolating the measured profiles to zero concentration. Note the logarithmic scale. (D) Two-component ellipsoid fit (black solid line) and scattering intensity recorded at 5 mM detergent concentration (magenta circles). The residuals of the fit are shown in the inset. Fitted parameters are presented in Table 2.

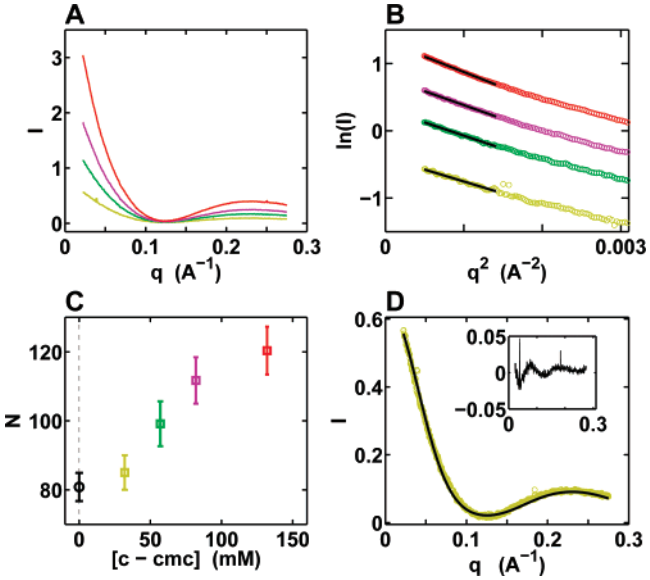

Figure 6. Scattering data, Guinier analysis, and two-shell ellipsoid fit for OG. (A) SAXS profiles ($I(q)$) of OG at detergent concentrations of 50 (brown), 75 (green), 100 (purple), and 150 (red) mM. (B) Guinier representation ($\ln(I)$ as a function of q^2) of the low angle data (same color code as part A) and Guinier fits (black lines). (C) Apparent aggregation numbers N obtained from the extrapolated forward scattering intensity and eq 4 (squares, same color code as in part A). The point at 0 mM (black circle) corresponds to the estimate obtained by linearly extrapolating the measured profiles to zero concentration. (D) Two-component ellipsoid fit (black solid line) and scattering intensity recorded at 50 mM detergent concentration (brown circles). The residuals of the fit are shown in the inset. Fitted parameters are presented in Table 2.

contact with the positively charged trimethylamine group. The core dimensions for FC-12 are larger than those for FC-10, by ~1.7 Å in the short dimensions and by about 5 Å along the a axis. The short core dimension b is smaller for DHPC than for FC-10 and FC-12, as can be expected from the shorter alkyl chains (see below). For FC-10, $N_{Guinier}$ and N_{core} are in excellent agreement, and smaller than the aggregation values obtained for FC-12. This is consistent with the general observation that N increases with alkyl chain length as discussed further below. For FC-12, N_{core} is slightly larger than $N_{Guinier}$, but the results agree reasonably within error and with the values reported by Arora and Tamm[40] (see Table 1).

DHPC is different from the other detergents in this study as it has two alkyl chains. Our model for DHPC is in qualitative agreement with the results of Lin et al.,[20] who found DHPC to be a prolate ellipsoid with $b = 7.8$ Å and $a = 24$ Å using SANS. Interestingly, in their model the head group layer thickness is significantly different in the a and b dimensions (6 and 10 Å, respectively). In contrast, we obtain similar values of ~3.5 Å for both t_a and t_b, in good agreement with the models for FC-10 and FC-12. These differences may be due to the different scattering properties of neutrons and X-rays, which may bias the fitted models. The values for $N_{Guinier}$ and N_{core} obtained for DHPC (Table 1) exhibit some variation but agree reasonably within experimental error and are in the same range as the values reported by Chou et al.[41] ($N = 27$) and Tausk et al.[42] ($N = 35$).

DM and DDM. The SAXS intensities for the maltosides are well fit by oblate ellipsoid models with parameters given in Table 2. Experimental and fitted scattering profiles are shown in Figures 4D and 5D. Varying t_a and t_b independently did not significantly improve the fit and gave values for t_b within 0.5 Å of t_a. Similarly, treating ρ_2 as a fitting parameter did not result in a significant change from the value computed from the head group volume and did not significantly improve the fit. The results for DDM are in excellent agreement with the findings of Dupuy et al., who modeled dodecyl-β-D-maltoside as a two-component oblate ellipsoid with a 14.1 Å semi-minor axis and two 28.2 Å semi-major axes for the core and a 6.2 Å outer shell of uniform thickness.[25] For DM the core is smaller than for DDM, the short dimension a by about 1.8 Å and the long dimension b by about 5 Å, while the thickness of the head group layer is unchanged. This is to be expected as the two detergents have the same head group, but DM has a shorter alkyl chain than DDM (see below). For DDM, $N_{Guinier}$, N_{core}, and the available literature values are in excellent agreement (see Table 1). For DM, N_{core} and $N_{Guinier}$ are in excellent agreement, but slightly larger than the value measured by Anatrace, Inc. (http://www.anatrace.com/). This discrepancy might be due to differences in solution conditions, which unfortunately are not explicitly stated for the Anatrace measurement.

OG, NG, and DG. The n-alkyl-glucosides, in particular OG, have been studied extensively with a range of methods.[21,23,26,43−47] An initial SANS study modeled OG micelles as spheres,[23] but subsequent work found them to be nonspherical.[43−45] Giordano et al. modeled OG micelles as monodisperse elongated one-component ellipsoids and found that the micelles grow significantly in the long dimension with increasing detergent concentration.[21] Furthermore, they observed interparticle repulsion effects for detergent concentrations ≥0.6 M. Zhang et al. obtained an extensive data set using both X-ray and neutron scattering over a large q range for n-heptyl-β-D-glucoside (HG), OG, and NG.[26] They tested a variety of models and found the best fit using an elongated two-component cylinder form factor. Their model accounts for polydispersity in cylinder height using a Shultz distribution and for fluctuations in the monomer

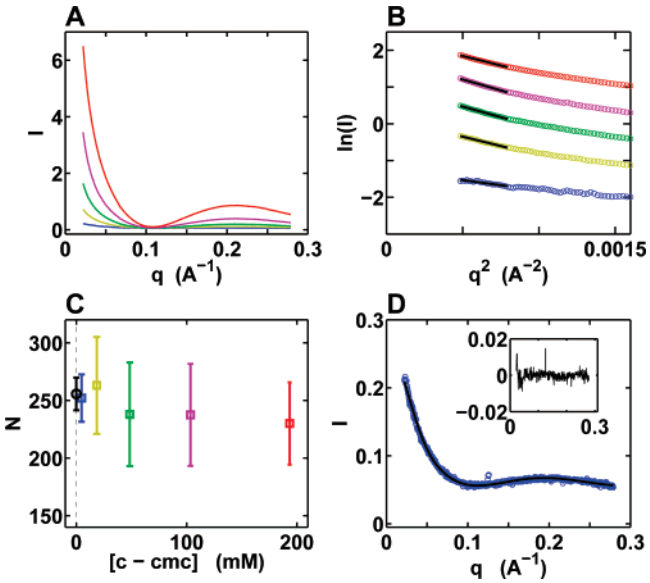

Figure 7. Scattering data, Guinier analysis, and two-shell ellipsoid fit for NG. (A) SAXS profiles ($I(q)$) of NG at detergent concentrations of 10 (blue), 25 (brown), 50 (green), 100 (purple), and 200 (red) mM. (B) Guinier representation (ln(I) as a function of q^2) of the low angle data (same color code as part A) and Guinier fits (black lines). (C) Apparent aggregation numbers N obtained from the extrapolated forward scattering intensity and eq 4 (squares, same color code as in part A). The point at 0 mM (black circle) corresponds to the estimate obtained by linearly extrapolating the measured profiles to zero concentration. (D) Two-component ellipsoid fit (black solid line) and scattering intensity recorded at 10 mM detergent concentration (blue circles). The residuals of the fit are shown in the inset. Fitted parameters are presented in Table 2.

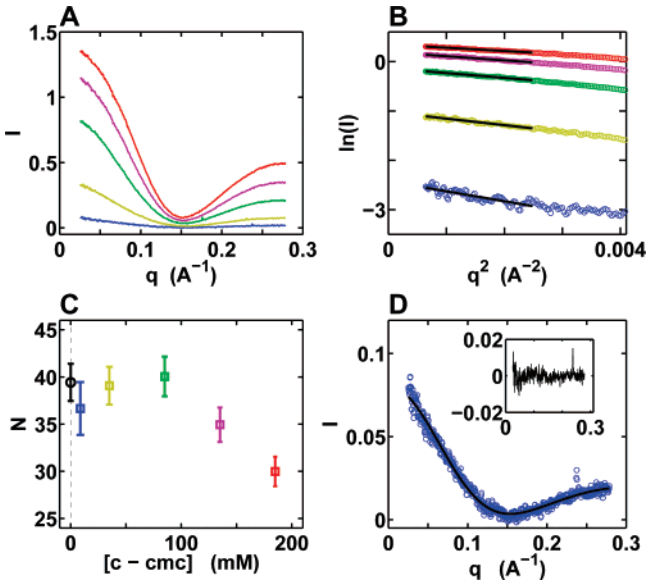

Figure 8. Scattering data, Guinier analysis, and two-shell ellipsoid fit for DHPC. (A) SAXS profiles ($I(q)$) of DHPC at detergent concentrations of 25 (blue), 50 (brown), 100 (green), 150 (purple), and 200 (red) mM. Profiles at 5 and 10 mM were recorded, but at these detergent concentrations below the cmc no scattering was detectable within experimental error. (B) Guinier representation (ln(I) as a function of q^2) of the low angle data (same color code as part A) and Guinier fits (black lines). (C) Apparent aggregation numbers N obtained from the extrapolated forward scattering intensity and eq 4 (squares, same color code as in part A). The point at 0 mM (black circle) corresponds to the estimate obtained by linearly extrapolating the measured profiles to zero concentration. (D) Two-component ellipsoid fit (black solid line) and scattering intensity recorded at 25 mM detergent concentration (blue circles). The residuals of the fit are shown in the inset. Fitted parameters are presented in Table 2.

positions by introducing a Debye−Waller factor-like formalism. The study found OG micelles to be significantly larger in D_2O than in H_2O and, in agreement with previous results, to grow along the long dimension with increasing detergent concentration.

HG, NG, and DG have been studied less extensively than OG, but the existing data suggest that they, too, form micelles with elongated, prolate, shapes. Zhang et al. modeled HG and NG similar to OG as polydisperse two-component cylinders and found HG to adopt much shorter (along the long dimension) and NG to adopt much more elongated micelles, compared to OG.[26] Their models suggest aggregation numbers of $N = 14$ for HG and of $N = 2700$ for NG, but the latter number is subject to considerable uncertainty. Nilsson et al. demonstrated that DG exhibits a complex phase diagram, which features phase separation into two liquid isotropic solutions for detergent concentrations from 3 to 500 mM.[46] For detergent concentration below 3 mM DG forms discrete micelles with an aggregation number in the range of 200−400.[46]

Instead of trying to replicate or improve on the comprehensive model by Zhang et al., we will use the scattering data for OG and NG micelles only to serve as a point of comparison with the other detergents. The scattering profiles for both OG and NG at different detergent concentrations are not superimposable after rescaling by (c − cmc) even for low concentrations, indicating a change in micelle size and shape with concentration and/or polydispersity of the size distribution. For simplicity, and to allow for direct comparison with the other detergents in this study, we fit the OG and NG scattering data using the two-component ellipsoid model outlined in the Material and Methods section. While Zhang et al. obtained better fits at high q using their two-component cylinder model, which includes polydispersity and a Debye−Waller factor, they found adequate fits with a two-component ellipsoid model for scattering data up to $q \approx 0.3$ Å^{-1}, which suggests that this simpler model is adequate for the range of q values considered here.

Our OG scattering data are reasonably fit by a prolate two-component ellipsoid model with parameters presented in Table 2 (see Figure 6D). Similar to Zhang et al., we find that the fitted thickness of the electron dense head group layer is dependent on the value used for the electron density of this region ρ_2. We find the best fit for $\rho_2 \approx 0.45$ e/Å^3 and $t_a = t_b \approx 4.5$−5.0 Å, which indicates that hydration effects are important for OG micelles. The short axes of the micelle are constant with increasing detergent concentration; however, the apparent length increases from $a \approx 40$ Å at 50 mM to 50−55 Å at 150 mM in reasonable agreement with the dimension determined in previous studies.[21,26,44]

The apparent aggregation number computed from the forward scattering intensity $N_{Guinier}$ increases with increasing OG concentration, consistent with micelle growth as a function of increasing c. For $c = 50$ mM $N_{Guinier} \approx 85$, in good agreement with the value of 87 obtained by Kameyama and Takagi[43] and slightly smaller than the value computed from the dimension of the fitted model $N_{core} \approx 100$.

Similar to OG, the NG scattering data can be reasonably modeled as a prolate two-component ellipsoid (see Figure 7D). Fitting parameter are presented in Table 2. Similar to the case of OG, the short b dimension is approximately constant and the micelles grow along the long a axis with increasing detergent concentration, from $a \approx 55$ Å at $c = 10$ mM to $a \approx 105$ Å at 50 mM. For even higher detergent concentration, the apparent micelle size decreases, which is likely a result of interparticle repulsion effects. The aggregation number determined from the

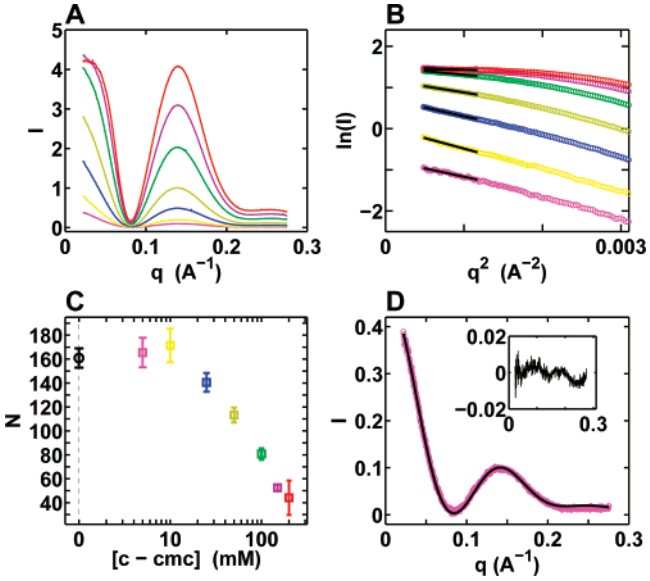

Figure 9. Scattering data, Guinier analysis, and two-shell ellipsoid fit for LPPG. (A) SAXS profiles ($I(q)$) of LPPG at detergent concentrations of 5 (magenta), 10 (yellow), 25 (blue), 50 (brown), 100 (green), 150 (purple), and 200 (red) mM. The effects of interparticle interference are clearly visible as a decrease in scattering intensity at low q in the 200 mM profile. (B) Guinier representation ($\ln(I)$ as a function of q^2) of the low angle data (same color code as part A) and Guinier fits (black lines). (C) Apparent aggregation numbers N obtained from the extrapolated forward scattering intensity and eq 4 (squares, same color code as in part A). The point at 0 mM (black circle) corresponds to the estimate obtained by linearly extrapolating the measured profiles to zero concentration. Note the logarithmic scale. (D) Two-component ellipsoid fit (black solid line) and scattering intensity recorded at 5 mM detergent concentration (magenta circles). The residuals of the fit are shown in the inset. Fitted parameters are presented in Table 2.

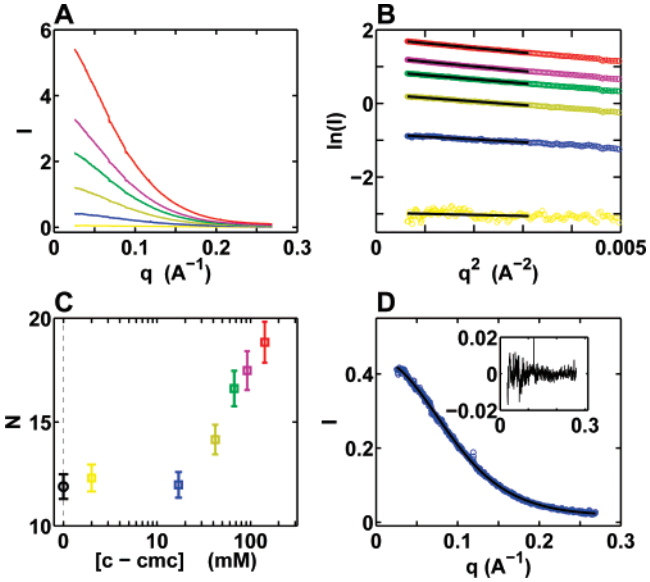

Figure 10. Scattering data, Guinier analysis, and one-component ellipsoid fit for CHAPS. (A) SAXS profiles ($I(q)$) of CHAPS at detergent concentrations of 10 (yellow), 25 (blue), 50 (brown), 75 (green), 100 (purple), and 150 (red) mM. (B) Guinier representation ($\ln(I)$ as a function of q^2) of the low angle data (same color code as part A) and Guinier fits (black lines). (C) Apparent aggregation numbers N obtained from the extrapolated forward scattering intensity and eq 4 (squares, same color code as in part A). The point at 0 mM (black circle) corresponds to the estimate obtained by linearly extrapolating the measured profiles to zero concentration. Note the logarithmic scale. (D) One-component ellipsoid fit (black solid line) and scattering intensity recorded at 25 mM detergent concentration (blue circles). The residuals of the fit are shown in the inset. Fitted parameters are presented in Table 2.

forward scattering intensity N_{core} shows a similar trend; however, the experimental error for the Guinier fits is considerable (see Figure 7C). Varying ρ_2 as an independent parameter improves the fit slightly and yields ρ_2 values lower than those computed from the head group volume alone, which might indicate that hydration effects are important. Similar to OG, the fitted thickness of the head group layer depends on the value for ρ_2, with lower values of ρ_2 giving rise to larger values for $t_a = t_b$. Varying t_a and t_b independently did not significantly improve the fit.

We also attempted measurements of DG; however, the viscosity and limited solubility of the detergent made handling and accurate adjustment of the detergent concentration difficult. Furthermore, interpretation of the data is complicated by the complex DG phase diagram as discussed above. Therefore, we limit the analysis of the DG scattering data to the determination of position of the second maximum in the scattering intensity, as discussed in the Second Peak' subsection.

LPPG. LPPG is the only ionic detergent in this study. For high detergent concentrations strong interparticle interference is observed (see the Guinier Analysis' subsection and Figure 9), which is likely attributable to electrostatic repulsion between micelles. However, for low detergent concentrations (≤25 mM) the scattering profiles are superimposable after scaling by (c − cmc) and are well described by an oblate form factor model (see Figure 9). Fitting parameters are presented in Table 2. Interestingly, variation of ρ_2 as an independent parameter did significantly improve the fit and yielded values of ρ_2 lower than those computed from the volume and chemical composition of the head group. This behavior suggests that hydration effects and interactions with the counterion cloud are more significant for this ionic detergent than for the non-ionic detergents considered in this study. Analysis of both the hydrophobic core volume and the forward scattering intensity gives aggregation numbers of 160−170 (Table 1). This value is larger than the aggregation number of ∼125 reported by Chou et al.[41] This difference can be at least qualitatively attributed to the fact that our measurements are done in the presence of 150 mM NaCl, whereas the study of Chou et al. used 20 mM phosphate buffer only, since addition of monovalent salt is known to increase the aggregation number for ionic detergents.[48]

CHAPS. CHAPS is the only amphiphile in this study that has a steroidal group instead of an alkyl chain as its hydrophobic moiety. The previous arguments about the hydrophobic core volume are, therefore, not directly applicable. Furthermore, there is no second maximum in the scattering intensity in the measured q range (see Figure 10A), suggesting that for CHAPS the contrast difference between hydrophobic core and hydrophilic head groups is much less pronounced than that for the other detergents. Therefore, we attempt to fit the SAXS pattern for CHAPS using one-component sphere and one-component ellipsoid models, i.e., formally using eq 7 with $\rho_2 = \rho_s$. While it is possible to fit a two-component model to the data, we find that the CHAPS scattering profile is well fit by a one-component prolate ellipsoid model (see Figure 10D), suggesting that this is the minimal model that can account for the data.

The apparent aggregation number derived from the forward scattering intensity increases for CHAPS with increasing detergent concentration (see the Guinier Analysis' subsection and Figure 10C) is similar to the behavior observed for OG micelles. In addition, the fitted dimensions of the micelle from the one-component ellipsoid model increase with increasing detergent concentration. The fitted value for the short dimension

TABLE 2: Geometrical Parameters of Detergent Micelles Obtained from the Two-Component Ellipsoid Fits

		parameters								
detergent[a]	shape	ρ_1 (e/Å^3)	ρ_2 (e/Å ^{3})	a (Å)	b (Å)	t_a (Å)	t_b (Å)	ϵ	a/b	R_g (Å)
FC-10	prolate	0.273	0.490	20.7−21.2	13.4−13.6	2.7−3.0	$\approx t_a$	0.76	1.55	25
FC-12	prolate	0.277	0.490	25.5−27.5	16.0−16.5	2.6−3.0	$\approx t_a$	0.80	1.63	34
DM	oblate	0.273	0.520	12.0−12.5	23.0−24.0	6.0−6.3	$\approx t_a$	0.85	0.52	26
DDM	oblate	0.277	0.520	13.8−14.3	28.0−29.5	6.0−6.3	$\approx t_a$	0.88	0.48	33
OG (50 mM)	prolate	0.268	0.45−0.54	39.0−42.0	12.0−13.2	3.2−5.0	$\approx t_a$	0.95	3.21	29
NG (10 mM)	prolate	0.271	0.50−0.53	55.0−60.0	13.5−15.0	4.0−5.2	$\approx t_a$	0.97	4.00	40
DHPC	prolate	0.253	0.464	20.5−22.5	9.5−10.0	3.0−4.0	$\approx t_a$	0.89	2.20	20
LPPG	oblate	0.281	0.46−0.48	19.0−20.0	29.5−30.5	5.5−6.0	$\approx t_a$	0.76	0.65	38
CHAPS [b] (25 mM)	prolate	n.a.	n.a.	31.0	10.5	n.a.	n.a.	0.94	2.95	15.4

[a] For all detergents, except for OG and DG, similar parameters were obtained from fits to the two or three lowest concentration profiles. [b] For CHAPS, a one-component ellipsoid model was fit to the scattering data (see text).

b increases from 10.5 Å at 50 mM CHAPS to 13.5 Å at 150 mM CHAPS, and the long dimension increases from ∼30 to ∼40 Å in the same concentration range. An increase in apparent micelle size could in principle be the result of attractive interparticle interactions or of true micelle growth with increasing detergent concentration. The fact that we find an increase in apparent micelle size at relatively low detergent concentrations (≤50 mM) suggests that CHAPS micelles indeed grow with increasing detergent, but we cannot rule out a convolution of the two effects.

The aggregation number determined from forward scattering $N_{core} \approx 11-12$ at a detergent concentration of 25 mM is in good agreement with the value determined by Hjelmeland et al. ($N = 10$), but slightly lower than the value computed from the volume of the prolate ellipsoid model divided by the volume of the monomer (Table 1). However, modeling the CHAPS micelle as a one-component ellipsoid neglects the effects of hydration as well as differences in scattering density in the micelle, both of which would increase the apparent aggregation number of the model.

Second Peak. The detergents investigated in this study (with the only exception of CHAPS) have a characteristic second peak in the scattering intensity, which stems from the large difference in scattering contrast between the detergent head groups and the aliphatic micelle core. A second maximum in the scattering intensity, in addition to the (first) maximum at $q = 0$ for forward scattering, is generally characteristic of core−shell structures.[49,50]

The position of the maximum at intermediate q is independent of detergent concentration (see Figures 2A−10A) and will be denoted with q_{max}. The peak position q_{max} corresponds to a length scale that is given by $2\pi/q_{max}$. Figure 11A shows the length scale $2\pi/q_{max}$ as a function of the number of alkyl carbons n_c for all detergents investigated in this study, except CHAPS. The maximum extension of an alkyl chain of length n_c is approximately[38] $l_c = (1.5 + 1.265n_c)$ Å and the maximal thickness across the alkyl core along the short dimension is $2l_c$. $2l_c$ (Figure 11A, solid black line) correlates well with the position of the second peak and the characterstic spacing $2\pi/q_{max}$ (Figure 11A, symbols) is consistently slightly larger than $2l_c$. This observation can be rationalized as follows: The second peak position is determined by the scattering interference between the electron dense head groups across the low electron density hydrophobic core. For an elongated micelle, there are in principle a range of head group−head group distances across the hydrophobic core. However, the dominant head group−head group distance is the short micelle dimension, as there are more monomers separated approximately by the short dimension than by other distances, for both prolate and oblate ellipsoids. The spacing from center to center of the head group layers across the short dimension of the micelle is approximately $d = 2a + t_a$ for oblate and $d = 2b + t_b$ for prolate ellipsoids. The distance d correlates well with the characteristic length scale $2\pi/q_{max}$ ($r = 0.95$) as shown in Figure 11 B.

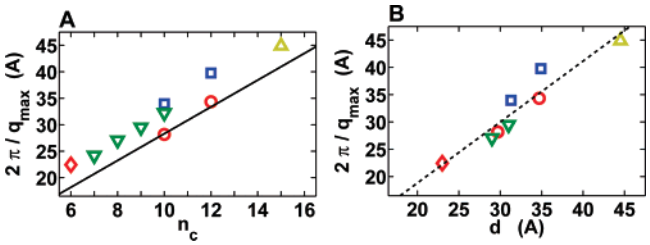

Figure 11. Characteristic head group−head group spacing determined from the position of the second maximum (q_{max}) of the scattering intensity. (A) Measured values for $2\pi/q_{max}$ are shown as a function of the number of alkyl carbons n_c for FC-10/12 (red ○), DM/DDM (blue □), *n*-heptyl-β-D-glucoside (HG)/OG/NG/DG (green ▽), DHPC (red ◊), and LPPG (brown △). The black line indicates the maximum extension of the alkyl chains[38] given by $2 \times (1.5 + 1.265n_c)$. The value for HG was taken from Figure 7 of Zhang et al.[26] (B) Measured values for $2\pi/q_{max}$ as a function of the head group−head group spacing d determined from the two-component ellipsoid fits (see text) for FC-10/12 (red ○), DM/DDM (blue □), OG/NG (green ▽), DHPC (red ◊), and LPPG (brown △). A linear regression with d as the independent variable gives a y-intercept of −3.5 Å and a slope of 1.1 (dashed line). The correlation coefficient is $r = 0.95$. CHAPS does not have an alkyl chain and does not exhibit a second peak in the scattering intensity and is, therefore, not included in the graph.

Trends in Micelle Size and Shape. The observed trends in aggregation number N and micellar shape can be qualitatively understood from theories of micelle formation.[12,38,51,52] Micelle formation is governed by two contributions to the free energy. The burial of the hydrophobic moieties in the lipid-like hydrophobic micelle core has a favorable (and mostly entropic[38]) contribution to the free energy that can be estimated from the free energy of transfer of the hydrophobic group from a lipid to the aqueous phase. This effect alone would favor very large aggregates and phase separation. However, since the hydrophilic head groups are covalently attached to the hydrophobic tails, micelle formation brings head groups into close proximity, which is energetically unfavorable and balances the hydrophobic effect. This balance of "opposing forces"[38] causes many amphiphiles (including the detergents in this study) to form micelles of a finite size. Several approaches have been proposed to quantitatively model head group−head group intercations. For ionic detergents electrostatic repulsion is important, but a theoretical treatment is complicated by the effect of screening counterions.[38,51] For non-ionic detergents entropic contributions

are suggested to be dominant and have been modeled in analogy to electrostatics.[12] More recently, even more sophisticated models have been developed,[52] which in part rely on extensive computer simulations to calibrate parameters.[13,53]

For a given head group, increasing the alkyl chain length favors larger aggregation numbers,[12,38] as the hydrophobic effect from packing the tail groups in the micelle interior become stronger (by ~0.8 kcal/mol per CH_2 group[38]). In agreement with this prediction, the observed aggregation numbers increase with increasing chain length for the maltoside sequence octyl-β-D-maltoside ($N = 21-25$[27]), DM ($N \approx 85$, Table 1), DDM ($N \approx 140$, Table 1), and tetradecyl-β-D-maltoside ($N \geq 1000$ [54]), and from DHPC (~35, Table 1) to 1,2-diheptanoyl-*sn*-glycero-phosphocholine ($N = 42$[8]). This prediction is also borne out by the newly determined aggregation numbers: FC-10 has a smaller N than FC-12 (~50 vs ~70, Table 1) and FC-14 ($N = 124$ [55]). Similarly, the aggregation number for NG (~250) is larger than that of OG (100) and HG (~14[26]). The elegant treatment by Chandler and co-workers based on the assumption of spherical micelle geometry[12] predicts an increase in aggregation number with alkyl chains length proportional to n_c^2. The phosphocholines follow this prediction approximately; however, the other micelles investigated in this study exhibit a more rapid increase of their aggregation number with alkyl chain length, which can likely be attributed to their pronouncedly nonspherical geometry (see below and Table 2).

An important constraint on the micelle shape is the maximum possible extension of the hydrocarbon chain, $l_c = (1.5 + 1.265n_c)$ Å for a n_c alkyl carbon[38] (see the Second Peak subsection). Since there cannot be a "hole'' in the middle of the micelle, one dimension of the micelle is always limited by this extension. Furthermore, this constraint sets an upper limit, $N_{max,sph}$, to the aggregation number consistent with spherical geometry for micelles with a certain alkyl chain length, $N_{max,sph} = (4\pi/3)l_c^3/V_{tail}$, as emphasized by Israelachvili et al.[51] For all detergents included in this study $N > N_{max,sph}$, in agreement with the observation that spherical models are unable to account for the scattering data. Indeed, the data are well described by two-component ellipsoid models, with short dimensions for the micelle core (a for oblate and b for prolate ellipsoids) that are consistently close to, but smaller than the maximum extension l_c (see the Second Peak subsection).

Since the short dimension of the micelle is constrained by l_c, increasing the number of alkyl carbons for a fixed head group has two effects on the micelle shape: The micelle grows in the short dimension by about 1.0 to 1.5 Å per additional alkyl group, due to the longer alkyl chain. The additional growth related to an increase in N (dicussed above) occurs primarily along the long dimension, which leads to more elongated micelle shapes, reflected in smaller (larger) values for a/b for oblate (prolate) ellipsoids and larger values of the ellipticity ϵ with increasing n_c. Both trends are borne out by the data for the maltosides, glucosides, and phosphocholines (see Table 2).

Israelachvili et al. show that, under fairly general assumptions about the form of the chemical potential, long cylindrical, "rod-like" micelles are predicted to exhibit larger polydispersity in their size distribution and a stronger dependence of the aggregation number on detergent concentration than more spherical or oblate micelles. In agreement with this prediction, the detergents with the most prolate or "rod-like" micelles in the study, the glucosides and CHAPS, exhibit signs of polydispersity and show a stronger dependence of their aggregation numbers on detergent concentration than the other detergents in this work.

Comparison of micelles formed by detergents with the same hydrophobic tail and different head groups requires consideration of the head group−head group repulsion. A comparison of the non-ionic maltosides (DM and DDM) to the zwitterionic phosphocholines of the same chain length (FC-10 and FC-12) shows that the phosphocholines have smaller aggregation numbers, which can be rationalized by the stronger repulsive forces between the more polar head groups of the zwitterions. Comparing non-ionic detergents, the glucosides exhibit larger aggregation numbers and less spherical micelles compared to the maltosides for the same chain length. A likely explanation is that the larger head group of the maltosides as compared to the glucosides leads to stronger steric repulsion and, therefore, to smaller micelles (which, as a result, are more spherical).

Of all detergents in this study, LPPG has the longest alkyl chain ($n_c = 15$) and is the only detergent with a charged head group. The long alkyl chain alone would predict the formation of very large micelles; however, the strong electrostatic repulsion between the ionic head groups alone would lead to the expectation of much smaller micelles compared to non-ionic detergents with a similar length alkyl chain. Apparently, the two effects balance such that the observed aggregation number for LPPG is comparable to the other detergents in this study.

Another interesting case is DHPC, the only detergent in this study with two alkyl chains. DHPC has a shorter alkyl chain than the other detergents in this study ($n_c = 6$), which would suggest a very small aggregation number (and a very high cmc). However, the fact that there are two alkyl chains per head group partially compensates for the short alkyl chains, and DHPC forms micelles with a size and cmc comparable to other detergents in this study. The shortest distance across the micelle core is still limited by the maximum extent of the individual chains, though, and consequently DHPC forms the micelles with the shortest distance d (see above) of the detergents in this study.

The behavior of CHAPS is more difficult to predict, as CHAPS has a rigid polycyclic ring structure as the hydrophobic region of the amphiphile. Experimentally, we find that CHAPS forms relatively small micelles, which is likely a consequence of its specific steric constraints.

In summary, simple theories of micelle formation are sufficient to rationalize the observed trends in micelle sizes and shapes qualitatively. However, there is currently no general theory that achieves accurate quantitative predictions of micelle shape and aggregation number N from first principles. The lack of a truly predictive theory highlights the need for accurate experimental determination of micelle parameters.

Conclusions

The present study of nine detergents commmonly used to solubilize membrane proteins is similar in spirit to previous works employing small-angle scattering techniques to provide insights into the structure and interactions of detergent micelles. The general approach in these studies has been to use simple geometric form factor models, such as two-component spheres,[18] ellipsoids,[19,20,22,25] or cylinders,[26] for the micelle structure. Some of the studies have included finite concentration interparticle interference effects explicitly using simple models for interparticle interactions.[19,33,34,56] In this study, we use a two-component ellipsoid model for the micelle structure and, in addition, present two novel and complementary analyses of the scattering data. As the focus of this work is on micelle structure, we only discuss the effect of micelle interactions qualitatively and limit the form factor modeling to conditions where interparticle interference is negligible.

The two-component ellipsoid model for the scattering intensities is clearly still a crude approximation to real detergent

micelles. It neglects molecular detail, fluctuations, and possible polydispersity. However, it provides a reasonable intermediate scale model and appears to be the minimal model that can account for the observed scattering profiles. In particular, none of the detergents measured in this study could be plausibly fit by using strictly spherical models. Furthermore, we find that one-component ellipsoid models fail to reproduce the characteristic second maximum in the scattering intensity, which is observed for all detergents but CHAPS.

Using Guinier analysis of the low q scattering data, we obtain an independent measurement of the forward scattering intensity and radius of gyration. The Guinier approach requires no assumptions about the micelle geometry. The radii of gyration obtained directly from Guinier analysis agree well with the values computed from the ellipsoidal form factor models (see Tables 1 and 2). The extrapolated forward scattering intensity can be used to obtain an independent measurement of the micellar aggregation number N_{Guinier}. The values for N_{Guinier} agree favorably with the aggregation numbers computed from the ellipsoidal models (see Table 1) and provide a consistency check on the form factor models. Furthermore, the Guinier approach in combination with the values for ρ_{det} tabulated in Table 1 can be applied to protein−detergent complexes, to obtain the oligomerization state of proteins inside of a detergent micelle.[2,9]

The position of the second peak q_{max} provides a straightforward and robust measure of the characteristic detergent spacing across the short micelle dimension. Recent results indicate that this spacing is a critical determinant of protein structure and dynamics in PDCs and that the position of the second peak provides a convenient way to evaluate the detergent packing in mixed micelles.[10]

This study provides a compilation of data that we anticipate to be useful both for experimentalists interested in studies of membrane proteins as well as for theoreticians trying to improve on existing models of micellation.[12,13] Finally, the analyses presented here are easily generalizable to other micelle forming detergents and to mixed micelles.

Acknowledgment. The authors thank Sönke Seifert for help with the data collection at the APS, Ian S. Millett for help and discussions in the initial stages of this project, Marc Delarue for useful discussions, and Yu Bai for providing the DNA duplex molecular weight standard. This research was supported by National Science Foundation Grant PHY-0140140, National Institutes of Health grants PO1 GM0066275 and 1F32GM068286, and National Institutes of Health Protein Structure Initiative grants P50 GM62411 and U54 GM074898. Use of the Advanced Photon Source was supported by the U.S. Department of Energy, Office of Science, Office of Basic Energy Sciences, under Contract No. DE-AC02-06CH11357.

References and Notes

(1) Eshaghi, S.; Hedrén, M.; Nasser, M. I. A.; Hammarsberg, T.; Thornell, A.; Nordlund, P. *Protein Sci.* **2005**, *14*, 676−683.

(2) Columbus, L.; Lipfert, J.; Klock, H.; Millett, I. S.; Doniach, S.; Lesley, S. *Protein Sci.* **2006**, *15*, 961−975.

(3) Sanders, C. R.; Sonnichsen, F. *Magn. Reson. Chem.* **2006**, *44*, 24−40.

(4) Marone, P. A.; Thiyagarajan, P.; Wagner, A. M.; Tiede, D. M. *J. Cryst. Growth* **1999**, *207*, 214−225.

(5) Wiener, M. C. *Methods* **2004**, *34* (3), 364−372.

(6) Berger, B. W.; Garcia, R. Y.; Lenhoff, A. M.; Kaler, E. W.; Robinson, C. R. *Biophys. J.* **2005**, *89* (1), 452−464.

(7) Roth, M.; Lewit-Bentley, A.; Michel, H.; Deisenhofer, J.; Huber, R.; Oesterhelt, D. *Nature* **1989**, *340*, 659−662.

(8) le Maire, M.; Champeil, P.; Moller, J. V. *Biochim. Biophys. Acta* **2000**, *1508* (1−2), 86−111.

(9) Lipfert, J.; Columbus, L.; Chu, V. B.; Doniach, S. *J. Appl. Crystallogr.* **2007**, *40*, S229−S234.

(10) Columbus, L.; Lipfert, J.; Doniach, S.; Lesley, S. A. **2007**. Submitted for publication

(11) Andersen, O. S.; Koeppe, R. E., II *Annu. Rev. Biophys. Biomol. Struct.* **2007**, *36*, 107−30.

(12) Maibaum, L.; Dinner, A. R.; Chandler, D. *J. Phys. Chem. B* **2004**, *108*, 6778−6781.

(13) Stephenson, B. C.; Goldsipe, A.; Beers, K. J.; Blankschtein, D. *J. Phys. Chem. B* **2007**, *111*(5), 1045−1062.

(14) Doniach, S. *Chem. Rev.* **2001**, *101*, 1763−1778.

(15) Svergun, D. I.; Koch, M. H. J. *Rep. Prog. Phys.* **2003**, *66*, 1735−1782.

(16) Koch, M. H. J.; Vachette, P.; Svergun, D. I. *Q. Rev. Biophys.* **2003**, *36* (2), 147−227.

(17) Lipfert, J.; Doniach, S. *Annu. Rev. Biophys. Biomol. Struct.* **2007**, *36*, 307−327.

(18) Hayter, J. B.; Zemb, T. *Chem. Phys. Lett.* **1982**, *93* (1), 91−94.

(19) Bendedouch, D.; Chen, S.-H.; Koehler, W. C. *J. Phys. Chem.* **1983**, *87*, 2621−2628.

(20) Lin, T.-L.; S.-H., C.; Gabriel, N. E.; Roberts, M. F. *J. Am. Chem. Soc.* **1986**, *108*, 3499−3507.

(21) Giordano, R.; Maisano, G.; Teixeira, J. *J. Appl. Crystallogr.* **1997**, *30*, 761−764.

(22) Bezzobotnov, V. Y.; Borbély, S.; Cser, L.; Faragó, B.; Gladkih, I. A.; Ostanevich, Y. M.; Vass, S. *J. Phys. Chem.* **1988**, *92*, 5738−5743.

(23) Thiyagarajan, P.; Tiede, D. M. *J. Phys. Chem.* **1994**, *98*, 10343−10351.

(24) Chen, S. H. *Annu. Rev. Phys. Chem.* **1986**, *37*, 351−399.

(25) Dupuy, C.; Auvray, X.; Petipas, C.; Rico-Lattes, I.; Lattes, A. *Langmuir* **1997**, *13*, 3965−3967.

(26) Zhang, R.; Marone, P. A.; Thiyagarajan, P.; Tiede, D. M. *Langmuir* **1999**, *15*, 7510−7519.

(27) He, Z.; Garamus, V. M.; Funari, S. S.; Malfois, M.; Willumeit, R.; Niemeyer, B. *J. Phys. Chem. B* **2002**, *106*, 7596−7604.

(28) Hayter, J. B. *Proc. Int. Sch. Phy. "Enrico Fermi"* **1985**, *90*, 59−92.

(29) Lipfert, J.; Millett, I. S.; Seifert, S.; Doniach, S. *Rev. Sci. Instrum.* **2006**, *77*, 046108.

(30) Beno, M. A.; Jennings, G.; Engbretson, M.; Knapp, G. S.; Kurtz, C.; Zabransky, B.; Linton, J.; Seifert, S.; Wiley, C.; Montano, P. A. *Nucl. Instrum. Methods Phys. Res., Sect. A* **2001**, *467*−*468*, 690−693.

(31) Seifert, S.; Winans, R. E.; Tiede, D. M.; Thiyagarajan, P. *J. Appl. Crystallogr.* **2000**, *33*, 782−784.

(32) Bai, Y.; Das, R.; Millett, I. S.; Herschlag, D.; Doniach, S. *Proc. Natl. Acad. Sci. U.S.A.* **2005**, *102* (4), 1035−1040.

(33) Hayter, J. B.; Penfold, J. *Mol. Phys.* **1981**, *42* (1), 109−118.

(34) Kotlarchyk, M.; Chen, S. H. *J. Chem. Phys.* **1983**, *79* (5), 2461−2469.

(35) Guinier, A. *Ann. Phys.* (*Paris*) **1939**, *12*, 161−237.

(36) Glatter, O.; Kratky, O. *Small Angle X-Ray Scattering*; Academic Press: London, UK, 1982.

(37) Schiel, J. E.; Hage, D. S. *Talanta* **2005**, *65* (2), 73341−73346.

(38) Tanford, C. *The hydrophobic effect*: *formation of micelles and biological membranes*, 2nd ed.; Wiley: New York, 1980.

(39) Reynolds, J. A.; McCaslin, D. R. *Methods Enzymol.* **1985**, *117*, 41−53.

(40) Arora, A.; Tamm, L. K. *Curr. Opinion Struct. Biol.* **2001**, *11*.

(41) Chou, J. J.; Baber, J. L.; Bax, A. *J. Biomol NMR* **2004**, *29* (3), 299−308.

(42) Tausk, R. J.; van Esch, J.; Karmiggelt, J.; Voordouw, G.; Overbeek, J. T. *Biophys. Chem.* **1974**, *1* (3), 184−203.

(43) Kameyama, K.; Takagi, T. *J. Colloid Interface Sci.* **1990**, *137* (1), 1−10.

(44) He, L.-Z.; Garamus, V.; Niemeyer, B.; Hemlholz, H.; Willumeit, R. *J. Mol. Liq.* **2000**, *89*, 239−249.

(45) Nilsson, F.; Söderman, O.; Johansson, I. *Langmuir* **1996**, *12*, 902−908.

(46) Nilsson, F.; Söderman, O.; Hansson, P.; Johansson, I. *Langmuir* **1998**, *14*, 4050−4058.

(47) Ericsson, C. A.; Soderman, O.; Garamus, V. M.; Bergstrom, M.; Ulvenlund, S. *Langmuir* **2004**, *20* (4), 1401−1408.

(48) Quina, F. H.; Nassar, P. M.; Bonilha, J. B. S.; Bales, B. L. *J. Phys. Chem.* **1995**, *99*, 17028−17031.

(49) Schurtenberger, P.; Jerke, G.; Cavaco, C.; Pedersen, J. S. *Langmuir* **1996**, *12*, 2433−2440.

(50) Bagger-Jörgensen, H.; Olsson, U.; Mortensen, K. *Langmuir* **1997**, *13*, 1413−1421.
(51) Israelachvili, J. N.; Mitchell, D. J.; Ninham, B. W. *J. Chem. Soc. Faraday II* **1976**, *72*, 1525−1568.
(52) Nagarajan, R.; Ruckenstein, E. *Langmuir* **1991**, *7*, 2934−2969.
(53) Stephenson, B. C.; Goldsipe, A.; Beers, K. J.; Blankschtein, D. *J. Phys. Chem. B* **2007**, *111* (5), 1025−1044.
(54) Ericsson, C. A.; Soderman, O.; Garamus, V. M.; Bergstrom, M.; Ulvenlund, S. *Langmuir* **2005**, *21* (4), 1507−1515.
(55) Strop, P.; Brunger, A. T. *Protein Sci.* **2005**, *14*, 2207−2211.
(56) Hansen, J.-P.; Hayter, J. B. *Mol. Phys.* **1981**, *46*, 651−656.
(57) Lorber, B.; Bishop, J. B.; Delucas, L. J. *Biochim. Biophys. Acta* **1990**, *1023*, 254−265.
(58) Chattopadhyay, A.; London, E. *Anal. Biochem.* **1984**, *139* (2), 408−412.
(59) DeGrip, W. J.; Bovee-Geurts, P. H. M. *Chem. Phys. Lipids* **1979**, *23*, 321−335.
(60) Helenius, A.; McCaslin, D. R.; Fries, E.; Tanford, C. *Methods Enzymol.* **1979**, *56*, 734−749.
(61) Stafford, R. E.; Fanni, T.; Dennis, E. A. *Biochemistry* **1989**, *28* (12), 5113−5120.
(62) Hjelmeland, L. M.; Nebert, D. W.; Osborne, J. C., Jr. *Anal. Biochem.* **1983**, *130* (1), 72−82.